Immunity
Article

Selective Expression of the Chemokine Receptor XCR1 on Cross-presenting Dendritic Cells Determines Cooperation with CD8$^+$ T Cells

Brigitte G. Dorner,[1,4] Martin B. Dorner,[1,4] Xuefei Zhou,[1,4] Corinna Opitz,[1] Ahmed Mora,[1] Steffen Güttler,[1] Andreas Hutloff,[1] Hans W. Mages,[1] Katja Ranke,[1] Michael Schaefer,[2] Robert S. Jack,[3] Volker Henn,[1] and Richard A. Kroczek[1,*]
[1]Molecular Immunology, Robert Koch-Institute, 13353 Berlin, Germany
[2]Rudolf-Boehm-Institute of Pharmacology and Toxicology, 04107 Leipzig, Germany
[3]Institute of Immunology, University of Greifswald, 17489 Greifswald, Germany
[4]These authors contributed equally to this work
*Correspondence: kroczek@rki.de
DOI 10.1016/j.immuni.2009.08.027

SUMMARY

The expression of the chemokine receptor XCR1 and the function of its ligand XCL1 (otherwise referred to as ATAC, lymphotactin, or SCM-1) remained elusive to date. In the present report we demonstrated that XCR1 is exclusively expressed on murine CD8$^+$ dendritic cells (DCs) and showed that XCL1 is a potent and highly specific chemoattractant for this DC subset. CD8$^+$ T cells abundantly secreted XCL1 8–36 hr after antigen recognition on CD8$^+$ DCs in vivo, in a period in which stable T cell-DC interactions are known to occur. Functionally, XCL1 increased the pool of antigen-specific CD8$^+$ T cells and their capacity to secrete IFN-γ. Absence of XCL1 impaired the development of cytotoxicity to antigens cross-presented by CD8$^+$ DCs. The XCL1-XCR1 axis thus emerges as an integral component in the development of efficient cytotoxic immunity in vivo.

INTRODUCTION

In the immune system, intercellular communication is facilitated by chemokines. Structurally, chemokines can be grouped into the CX3C, CXC, CC, and C families (Zlotnik and Yoshie, 2000). Some of the chemokines are expressed constitutively and are involved primarily in the organization of lymphoid tissue ("homeostatic" chemokines), and others are mainly involved in the orchestration of an inflammatory response ("inflammatory" chemokines). Activation-induced, T cell-derived, and chemokine-related cytokine (ATAC), the only member of the C family of chemokines, was cloned by our laboratory (Müller et al., 1995), and independently as lymphotactin (Kelner et al., 1994) and SCM-1 (Yoshida et al., 1995), and was later given the official designation XCL1 (Zlotnik and Yoshie, 2000). XCL1, a polypeptide of 93 aa (Dorner et al., 1997), is secreted by CD8$^+$ T cells, Th1 cell-polarized CD4$^+$ T cells (Dorner et al., 2002), and NK cells (Dorner et al., 2004) upon activation. Cosecretion of XCL1 with IFN-γ and the inflammatory chemokines MIP-1α, MIP-1β, and RANTES by CD8$^+$ T cells and NK cells in several infection models strongly suggested that XCL1 is an integral part of the Th1 cell immune response (Dorner et al., 2002, 2004).

XCL1 has originally been described as a chemoattractant for thymocytes and T lymphocytes (Kelner et al., 1994; Kennedy et al., 1995), and later for a variety of other cell types, including B cells and NK cells, but this function could not be substantiated by others (Dorner et al., 1997; Yoshida et al., 1998; Bleul et al., 1996) (for an extensive list of positive and negative reports on chemotactic properties of XCL1, see Table S1 available online). XCR1 is the only receptor for XCL1 (Yoshida et al., 1998). In the absence of XCR1-specific antibodies, expression of XCR1 had to be measured by PCR and was reported in a variety of cell types, including T cells, B cells, and NK cells (see Table S2). However, apparent detection of XCR1 did not match the (disputed) function of XCL1 reported by others, so the role of XCL1 in the immune system remained elusive to date.

Dendritic cells (DCs) present antigen to naive T cells and thus prime them for immune function. "Migratory" DCs, among them interstitial DCs or Langerhans' cells, reside in the periphery, take up antigen there, and transport it to lymph nodes (LN) for presentation. "Resident" DCs, which make up the large majority of splenic and thymic DCs, take up antigen locally and present it to T cells "on site." Resident DCs, which all express the CD11c cell surface protein, can be subdivided into CD11b^{hi}CD4$^+$ CD8$^-$CD205^{lo} DCs ("CD4$^+$ DCs," around 70% of splenic DCs), CD11b^{lo}CD8$^+$CD205^{hi} DCs ("CD8$^+$ DC," 20%), and CD11b^{hi} CD4$^-$CD8$^-$CD205^{lo} DCs ("DN" DCs, 10%) (Vremec et al., 2000).

The relative roles of the various DC subtypes in antigen presentation is at present only partially understood, but it is clear that resident CD8$^+$ DCs are critically involved in antigen "cross-presentation," in which exogenous antigen is not "classically" presented in the context of MHC class II, but instead shunted to the MHC class I pathway. Cross-presentation to T cells (den Haan et al., 2000; Heath et al., 2004) has been shown to be of major importance in the defense against viral and bacterial pathogens, and also in the recognition of tumor antigens (Huang et al., 1994).

In the present report, we identified XCL1 as a potent chemokine with a selective action on CD8$^+$ DCs. These functional results are in line with extensive whole-body expression analyses strongly indicating an exclusive utilization of XCR1 by

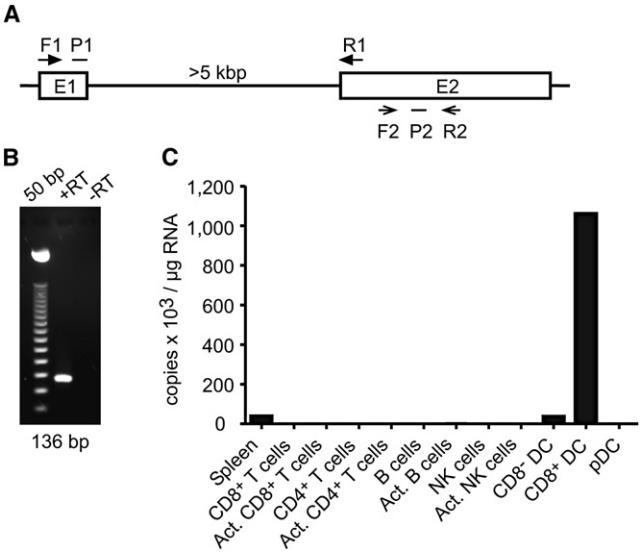

Figure 1. The Chemokine Receptor XCR1 Is Selectively Expressed in CD8+ DCs

(A) Organization of the murine *Xcr1* gene. E1, exon 1; E2, exon 2. Primer sets used for expression analyses are indicated.

(B) A PCR product of 136 bp obtained by standard RT-PCR of total RNA from spleen with primers F1 and R1. RT, reverse transcriptase.

(C) Quantitative RT-PCR of total RNA from C57BL/6 spleen, resting and activated $CD8^+$ and $CD4^+$ T cells, B cells, NK cells, resting $CD8^-$ DCs, $CD8^+$ DCs, and pDCs via primers F1, R1, and probe P1. An independent qRT-PCR performed with poly(A)RNA obtained from the same cells, and in addition from granulocytes (primers F2, R2, probe P2), gave identical results (data not shown).

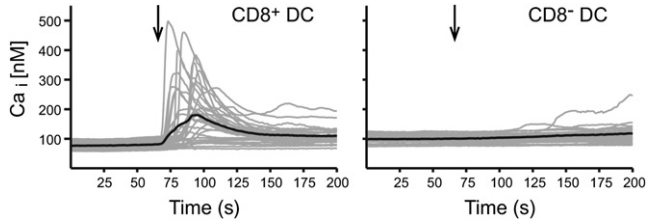

Figure 2. XCL1 Induces a $[Ca^{2+}]_i$ Signal in $CD8^+$, but Not in $CD8^-$, DCs

$CD8^+$ or $CD8^-$ DCs were flow-sorted to a purity >96%, immobilized on poly-L-lysine-coated glass coverslips, and loaded with fura-2/AM (2 µM). Cells were imaged in a monochromator-assisted digital video imaging system and challenged with 1000 ng/ml XCL1 as indicated (arrow). Data represent intracellular Ca^{2+} concentrations ($[Ca^{2+}]_i$) in 45–56 single cells (gray lines) measured in three independent experiments. Mean $[Ca^{2+}]_i$ signal averaged over all cells measured is indicated (black lines).

cross-presenting DCs. We provided evidence that $CD8^+$ T cells abundantly secrete XCL1 8–36 hr after encountering antigen on $CD8^+$ DCs and demonstrated that this XCL1 secretion is required for optimal expansion and differentiation of $CD8^+$ T cells to cytotoxic and IFN-γ-secreting cells in vivo.

RESULTS

The Chemokine Receptor XCR1 Is Selectively Expressed in $CD8^+$ DCs

All published data indicating a seemingly broad expression of murine or human XCR1 in the immune system (see Table S2) were obtained with total RNA and standard RT-PCR utilizing primers designed on the basis of the only exon known at that time (now exon 2). Recently, a new putative exon 1 for the murine XCR1 has been identified (Figure 1A, GenBank NC_000075). Analysis of splenic RNA by standard RT-PCR via primers F1 and R1 (Figure 1A) gave the expected product of 136 bp (Figure 1B) and thus demonstrated that XCR1 exon 1 is transcribed and spliced to exon 2. We thus could set up a highly sensitive and specific quantitative RT-PCR (qRT-PCR) spanning the large intron. This assay gave a very low XCR1 signal with total RNA obtained from C57BL/6 spleen, but no signal with RNA from highly purified resting or activated primary $CD8^+$ T cells, $CD4^+$ T cells, B cells, NK cells, or plasmacytoid DCs (pDCs) (Figure 1C). A strong XCR1 signal was obtained with RNA from $CD8^+$ DCs, and a very low signal with $CD8^-$ DCs (Figure 1C; for phenotypic definition of these populations see Figure 4A). Identical qualitative and quantitative results were obtained with an independent RT-qPCR system based on exon 2 only (Figure 1A), but only when poly(A)RNA was used instead of total RNA (indicating that previous reports on a broad expression of XCR1 were based on assays that were likely contaminated with genomic DNA). The same results were obtained with cells from BALB/c and 129SV mice (not shown). These experiments revealed, within the tested populations, an essentially selective expression of XCR1 mRNA in $CD8^+$ DCs.

XCL1 Mobilizes Calcium in $CD8^+$ DCs but Not in $CD8^-$ DCs

To test XCL1 for function on XCR1-bearing cells, primary splenic $CD8^+$ DCs and $CD8^-$ DCs were isolated to a purity >96% by flow sorting. When exposed to XCL1, $CD8^+$ DCs reacted by vigorous calcium mobilization, whereas $CD8^-$ DCs failed to respond under identical conditions (Figure 2). No calcium response was observed with $CD8^+$ DCs from homozygous B6.XCR1-lacZ mice, which lack the XCR1 receptor (not shown). These results indicated that XCR1 is expressed on the cell surface of $CD8^+$ DCs and also demonstrated the capacity of XCR1 to transduce an activation signal through binding of its chemokine ligand.

XCL1 Is a Chemoattractant for $CD8^+$ DCs, but Not for $CD8^-$ DCs, T Cells, B Cells, or NK Cells

To test XCL1 for chemotaxis, splenic DCs were enriched for $CD11c^+$ cells. The resulting population, containing approximately 23% $CD8^+$ DCs and 70% $CD8^-$ DCs (Figure 3A, "input DC"), exhibited only a low background migration in a transwell system. Upon addition of increasing amounts of XCL1, a selective migration of $CD8^+$ DCs was observed (Figure 3A). At the optimal concentration of XCL1 (100 ng/ml), more than 30% of all input $CD8^+$ DCs had migrated (Figures 3A and 3B), whereas less than 5% of the input $CD8^-$ DCs migrated under any of the conditions tested (Figure 3B). Controls with CCL21 ensured that the unresponsiveness of $CD8^-$ DCs to XCL1 was not caused by a general unresponsiveness of this DC subset (Figure 3B). Similar migration results were obtained with DC subsets from inguinal and popliteal LN (data not shown). Checkerboard

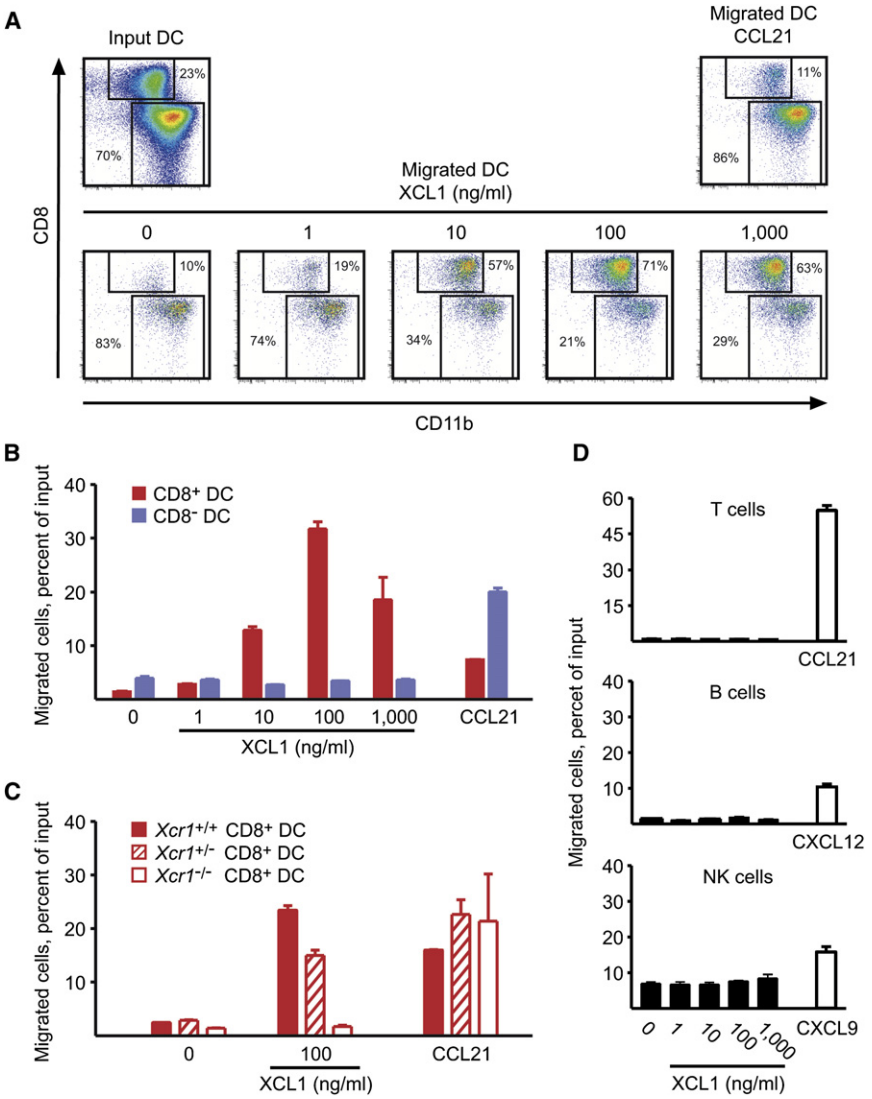

Figure 3. XCL1 Induces Chemotaxis via XCR1 in CD8+ DCs, but Not in CD8− DCs, T Cells, B Cells, or NK Cells

(A) Highly enriched splenic DCs (CD11c+ cells > 90%, "input DC") were tested for migration in response to medium alone or serial dilutions of XCL1 (1–1000 ng/ml) in a transwell system. The chemokine CCL21 (500 ng/ml) was used as a positive control for CD8− DCs. The input and migrated cell populations were analyzed for expression of CD8, CD11b, and CD11c by flow cytometry; shown are cells gated on CD11c. The absolute numbers of CD8+CD11b− DCs ("CD8+ DC") and CD8−CD11b+ DCs ("CD8− DC") in input and migrated cell populations are represented in the dot plots, because all cells were included in the analysis in each instance.

(B) Proportion of migrated CD8+ DCs and CD8− DCs relative to the input CD8+ DCs and CD8− DCs in the experiment shown in (A).

(C) Proportion of migrated wild-type CD8+ DCs ("*Xcr1*+/+ CD8+ DC"), heterozygous ("*Xcr1*+/− CD8+ DC"), and homozygous CD8+ DCs ("*Xcr1*−/− CD8+ DC") from B6.XCR1-lacZ mice in response to XCL1 (100 ng/ml).

(D) Proportion of migrated T cells, B cells, or NK cells in response to XCL1 (1–1000 ng/ml) or the chemokines CCL21 (100 ng/ml), CXCL12 (200 ng/ml), or CXCL9 (200 ng/ml) used as positive controls. All experiments were performed at least twice.

Data in (B)–(D) are presented as mean ± SEM.

analysis, performed by applying various dilutions of XCL1 in the lower and upper wells of the transwell system, indicated true chemotaxis and not only chemokinesis (not shown). The experiments shown were performed with chemically synthesized XCL1; identical results (not shown) were obtained with natural XCL1 (supernatants of a murine XCL1-transfectant or supernatants of activated CD8+ T cells). To exclude the involvement of another receptor mediating the XCL1-induced chemotaxis, we also tested DCs from mice in which the *Xcr1* gene has been replaced by a LacZ-reporter gene coding for β-galactosidase ("B6.XCR1-lacZ"). CD8+ DCs from heterozygous mice (containing one intact *Xcr1* allele) still exhibited substantial migration to XCL1, whereas CD8+ DCs from homozygous B6.XCR1-lacZ mice no longer responded (Figure 3C). In the literature, migration of T cells, B cells, and NK cells was repeatedly reported in response to XCL1. When we performed analogous transwell experiments, XCL1 failed to induce migration with any of these cell populations, whereas positive controls were effective (Figure 3D). Together, these experiments established that XCL1 is a chemokine that selectively attracts CD8+ DCs. Further, the results demonstrated that XCL1 exerts its chemotactic action exclusively through its receptor XCR1.

XCR1 Is Expressed in 70%–85% of Splenic CD8+ DCs

In order to determine whether XCR1 is expressed in all or only a subpopulation of CD8+ DCs, we further examined homozygous B6.XCR1-lacZ mice. Splenic cells were loaded with fluorescein-di-β-D-galactopyranoside (FDG) and analyzed by flow cytometry. A signal was routinely detected in 70%–85% of splenic CD8+ DCs (and highly correlated with CD103 and CD205) and in a small proportion (2%–8%) of CD4−CD8− DCs (associated to 50% with CD103 and correlated with CD205); all other splenic cell types, including CD4+ DCs, were negative (Figure 4A and not shown). Similar data were obtained with heterozygous LacZ reporter mice (not shown). Taken together, these LacZ-reporter data indicated that in the spleen, XCR1 is exclusively expressed in CD8+ DCs (70%–85%) and a small subset (2%–8%) of CD4−CD8− DCs.

Whole-Body Analysis Indicates Selective Expression of XCR1 in Cross-presenting Splenic DCs and Corresponding Cells in Other Organs

Flow cytometry and standard histological examination of homozygous B6.XCR1-lacZ reporter mice (lacking the XCR1 receptor) revealed an apparently undisturbed organ development and a normal immune cell composition, including DC subsets

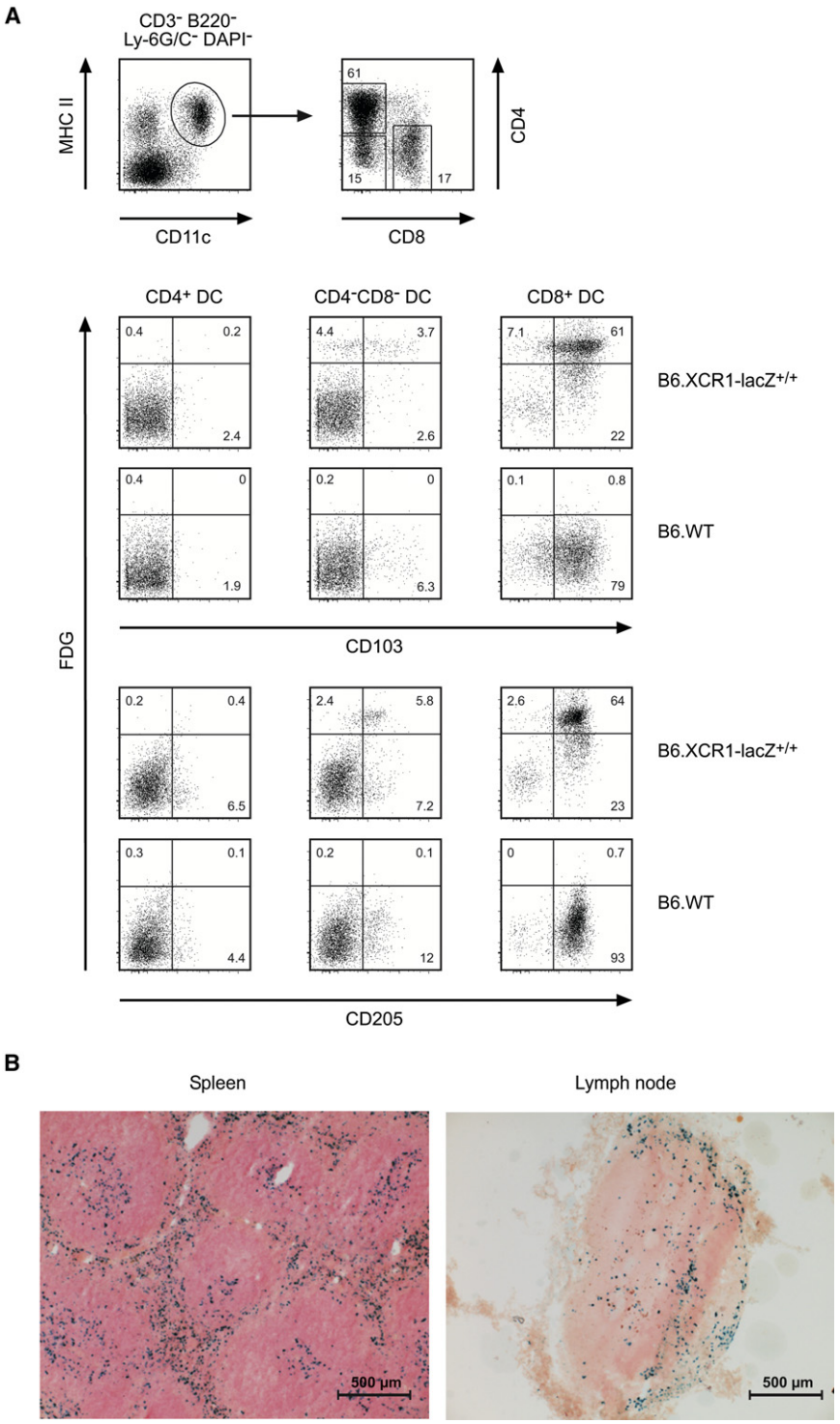

Figure 4. XCR1 Expression in the Spleen and Lymph Nodes

(A) Splenocytes from homozygous B6.XCR1-lacZ mice, in which both XCR1 genes are replaced by LacZ-reporter genes, were loaded with fluorescein-di-β-D-galactopyranoside (FDG), a fluorogenic substrate for β-galactosidase, and analyzed by flow cytometry. Various cell subsets were analyzed for FDG-fluorescence, shown are $CD11c^{hi}MHC\text{-}II^{hi}$ $CD4^+$ DCs, $CD4^-CD8^-$ DCs, and $CD8^+$ DCs, after staining for CD103 and CD205 (top rows, the inset numbers indicate percentage of cells). The background signal obtained after loading splenocytes from wild-type C57BL/6 mice with FDG is given in the lower rows. Shown is a representative experiment out of three. Identical results were obtained with heterozygous B6.XCR1-lacZ mice (not shown).

(B) XCR1 tissue distribution was determined in the spleen and the axillary lymph node of homozygous B6.XCR1-lacZ mice with X-gal, a chromogenic substrate for β-galactosidase. Similar results were obtained with heterozygous B6.XCR1-lacZ mice (not shown). No signals were detected in tissues of wild-type C57BL/6 animals.

(Table S3). Histochemical analysis of splenic tissue for β-galactosidase activity gave signals in the red pulp, the marginal zones, and in central areas of T cell zones (Figure 4B), and thus corresponded to the distribution of $CD8^+CD205^+$ DCs in the spleen (McLellan et al., 2002; Idoyaga et al., 2009). In lymph nodes, LacZ signals were identified in the subcapsular sinus and in the paracortical areas (Figure 4B). $LacZ^+$ cells were further found in all lymphoid tissues, where they represented a fraction of $CD11c^+$ cells (as determined in serial sections, not shown). A systematic analysis of nonlymphoid organs and tissues (see Experimental Procedures) revealed only very few $LacZ^+$ $CD11c^+$ cells, and their apearance and anatomical location suggested tissue-resident DCs. These histological results, when taken together with the qRT-PCR and the flow cytometry data, demonstrated that XCR1 expression in the mouse is essentially restricted to splenic $CD8^+$ DCs and to apparently similar cells in other lymphoid and nonlymphoid organs. Analogous data were obtained with heterozygous LacZ mice (not shown).

Normal Immune Cell Distribution in XCL1-Deficient Mice

To assess the overall biological role of the XCL1 chemokine-XCR1 receptor system in vivo, we generated *Xcl1*-deficient mice and backcrossed them to the C57BL/6 background. Homozygous $Xcl1^{-/-}$ mice no longer produced XCL1 mRNA or protein (see also Figure 5B). $Xcl1^{-/-}$ animals showed normal fertility and viability and had an apparently normal organ development and immune cell composition. More specifically, the frequency of DC subsets in the spleen and LN appeared normal (see Table S3). These results with $Xcl1^{-/-}$ mice, congruent with the data obtained with homozygous B6.XCR1-lacZ mice, indicated that XCL1 does not play a major role in the development

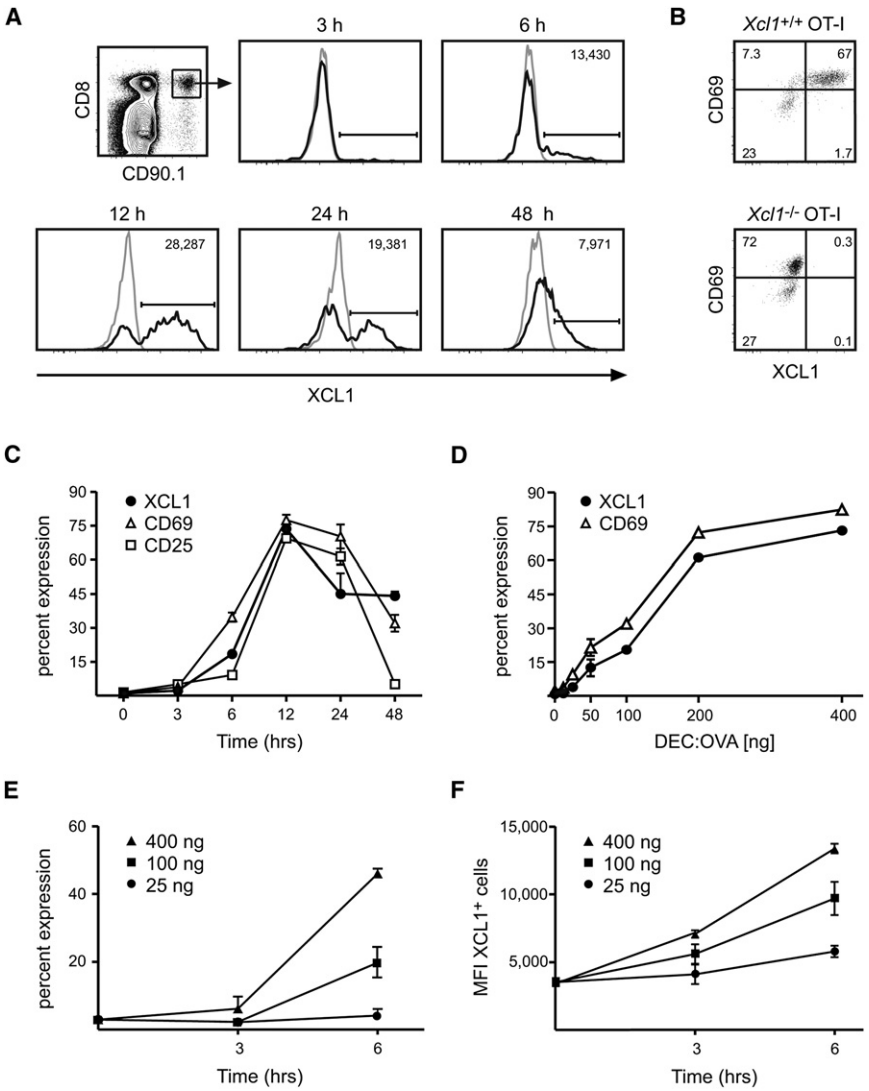

Figure 5. Kinetics and Dose Dependence of XCL1 Secretion by CD8+ T Cells upon Recognition of Antigen Presented by CD8+ DCs In Vivo

(A) OT-I T cells were transferred into syngeneic mice, 24 hr later the recipients were immunized by i.v. injection of 100 ng LPS-free αDEC-205:OVA and 6 μg CD40 mAb. XCL1 expression was analyzed in OT-I T cells (gated on the expression of the surface markers CD90.1 and CD8) from spleens removed at 3, 6, 12, 24, and 48 hr after immunization (bold histograms); background stainings obtained with *Xcl1*$^{-/-}$ OT-I T cells under the same conditions are represented by gray histograms. The inset numbers give the mean fluorescence intensity (MFI) of the signal in *Xcl1*$^{+/+}$ OT-I T cells.

(B) The correlation between the staining for XCL1 and CD69 in wild-type OT-I T cells ("*Xcl1*$^{+/+}$ OT-I," upper histogram) and *Xcl1*-deficient OT-I T cells ("*Xcl1*$^{-/-}$ OT-I," lower histogram) is detailed for the 12 hr time point.

(C) Proportion of XCL1-secreting wild-type OT-I T cells in the time-course experiment depicted in (A) correlated to the proportion of cells expressing the surface markers CD69 and CD25. Shown is a representative experiment of two.

(D) Proportion of XCL1-secreting OT-I T cells 8 hr after injection of increasing amounts of antigen (12.5, 25, 50, 100, 200, 400 ng αDEC-205:OVA).

(E) Time point of initial XCL1-secretion after injection of 25, 100, and 400 ng αDEC-205:OVA.

In experiments (D) and (E), αDEC-205:OVA was injected without the CD40 mAb.

(F) Mean fluorescence intensity (MFI) of the XCL1 signal in cells secreting this chemokine in the experiment shown in (E).

All experiments were performed at least twice. Data in (C)–(F) are presented as mean ± SEM.

and homeostatic positioning of XCR1-expressing cells in lymphoid tissues.

Antigen-Dependent Induction of XCL1 in CD8+ T Cells In Vivo

We analyzed the induction of the XCL1 chemokine protein in CD8+ T cells in vivo. OT-I T cells, bearing a transgenic T cell receptor for ovalbumin (OVA), were adoptively transferred into C57BL/6 syngeneic recipients. Twenty-four hours later, the recipients were injected i.v. with OVA coupled to a DEC-205-specific mAb (αDEC-205:OVA), thus targeting OVA to CD8+ DCs, together with a CD40 mAb, which induces maturation of DCs (Bonifaz et al., 2002). In preliminary experiments we had determined that XCR1 mRNA continues to be expressed under these immunization conditions (data not shown). Spleens were removed at defined time points and OT-I T cells were analyzed for secretion of XCL1 after incubation with Brefeldin A, but without further restimulation. XCL1 secretion started at around 6 hr after antigen delivery, peaked at 12 hr with around 75% of OT-I T cells secreting XCL1, and reached a plateau between 24 and 48 hr (Figures 5A and 5C). The kinetics of XCL1 secretion paralleled the expression of CD69 and CD25 on OT-I T cells (Figure 5C), and the three signals were highly correlated in single OT-I cells in the first 24 hr (Figure 5B, upper histogram, and not shown). The specificity of the intracellular staining for XCL1 was verified by comparing the signals in *Xcl1*$^{+/+}$ OT-I T cells (Figure 5A, black histograms) with signals in *Xcl1*$^{-/-}$ OT-I T cells (Figure 5A, gray histograms), as detailed for the 12 hr time point (Figure 5B). Interestingly, the percentage of OT-I T cells secreting XCL1 was dependent on the dose of antigen injected (Figure 5D), whereas the time point of initial XCL1 secretion was not (Figure 5E). The amount of XCL1 secreted per cell was correlated to the strength of the antigenic signal (Figure 5F). Overall, these experiments determined that activated CD8+ T cells secrete XCL1 over the entire period of time in which intense T cell-DC interactions occur (Mempel et al., 2004).

Absence of XCL1 Leads to a Decreased Pool Size of CD8+ T Cells Reacting to Antigen Cross-presented by CD8+ DCs

In order to examine any influence of XCL1 on CD8+ T cell priming and expansion under tolerizing and immunizing conditions,

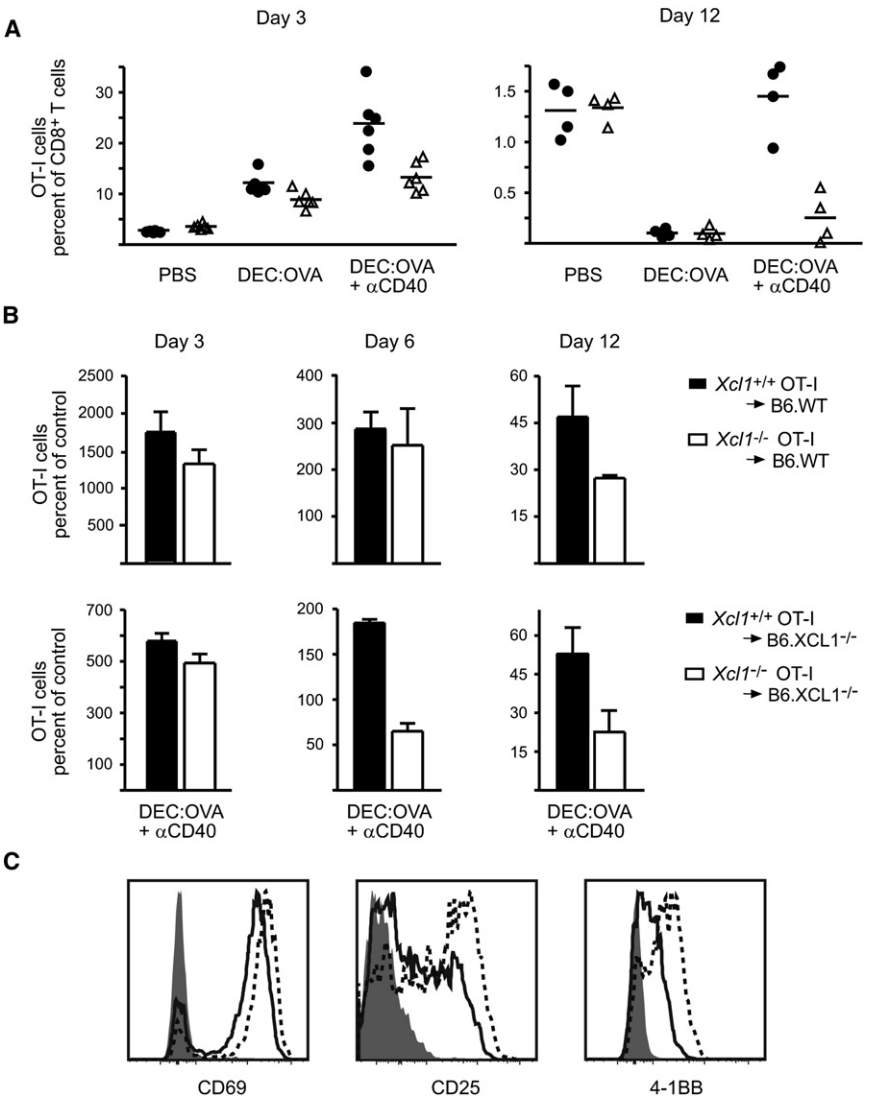

Figure 6. Influence of XCL1 on the Activation of T Cells Interacting with CD8+ DCs and Their Pool Size

(A) *Xcl1*$^{+/+}$ (filled circles) or *Xcl1*$^{-/-}$ (open triangles) OT-I T cells were adoptively transferred into wild-type or *Xcl1*-deficient recipients, respectively. Recipient animals were injected 24 hr later with αDEC-205:OVA or with αDEC-205:OVA in combination with CD40 mAb. Frequencies of OT-I T cells in spleens were determined on days 3 and 12 after antigen delivery. A representative experiment out of three is shown. The mean is indicated as a bar.

(B) *Xcl1*$^{+/+}$ or *Xcl1*$^{-/-}$ OT-I T cells were adoptively transferred into wild-type recipients (top row) versus *Xcl1*-deficient animals (bottom row) and their relative frequencies were determined on days 3, 6, and 12 after immunization with αDEC-205:OVA in combination with CD40 mAb (OT-I frequencies in PBS-injected animals = 100%). Representative experiment out of two. Data are presented as mean ± SEM.

(C) Expression of CD69, CD25, and 4-1BB on *Xcl1*$^{+/+}$ (bold histograms) versus *Xcl1*$^{-/-}$ (dotted histograms) OT-I T cells transferred into wild-type recipients, which were injected with αDEC-205:OVA. Shown are the flow cytometry profiles 20 hr after antigen delivery. Representative experiment out of six.

OT-I *Xcl1*$^{-/-}$ T cells and control OT-I T cells were transferred into *Xcl1*$^{-/-}$ C57BL/6 and wild-type C57BL/6 mice, respectively. Recipient mice were injected 24 hr later with LPS-free αDEC-205:OVA conjugate alone ("tolerization"), or with αDEC-205:OVA in combination with CD40 mAb ("immunization") (Bonifaz et al., 2002). Cell division analysis of OT-I *Xcl1*$^{+/+}$ and OT-I *Xcl1*$^{-/-}$ T cells via CFSE labeling and also analysis of apoptosis markers revealed some differences, but these were too small to allow clear conclusions. We therefore measured a functional end-point in the experimental system used, the size of the OT-I T cell pool. Three days after injection of αDEC-205:OVA alone, the frequency of *Xcl1*$^{-/-}$ OT-I T cells in the spleens of recipient animals was marginally reduced when compared to *Xcl1*$^{+/+}$ OT-I T cells (Figure 6A). However, upon injection of αDEC-205:OVA in combination with CD40 mAb, the difference in frequency rose to approximately 40% (Figure 6A). Twelve days after antigen delivery, at a time point when the initially expanded T cell population had contracted again, tolerization with αDEC-205:OVA reduced OT-I T cell numbers to a point that they were barely detectable, as described earlier (Bonifaz et al., 2002), and this effect was independent of XCL1 (Figure 6A). In contrast, after immunization with αDEC-205:OVA in combination with CD40 mAb, *Xcl1*$^{+/+}$ OT-I T cells could be detected at the expected frequency, whereas the number of *Xcl1*$^{-/-}$ OT-I T cells was drastically reduced (by an average of 74%), often to the point that they were no longer detectable (Figure 6A). Because the differences in the frequencies between the experimental groups could be caused by different kinetics of T cell egress from the spleen, we determined the presence of OT-I T cells in the immunization group in various organs on day 12. As shown in Table S4, the frequencies of *Xcl1*$^{-/-}$ OT-I T cells were highly reduced in all organs when compared to control OT-I T cells, indicating that the absence of XCL1 caused a substantial reduction of the antigen-reactive T cell pool on day 12.

We extended the experiments to control for any contribution of other cells secreting XCL1 and for any functional changes in CD8+ DCs in *Xcl1*$^{-/-}$ animals. First, we transferred *Xcl1*$^{+/+}$ OT-I versus *Xcl1*$^{-/-}$ OT-I T cells into wild-type recipients and compared their frequencies in the spleen 3, 6, and 12 after antigen injection. The frequencies of *Xcl1*$^{-/-}$ OT-I cells did not differ substantially at 3 and 6 days, but were reduced by about 40% on day 12 (Figure 6B, top row). Upon transfer into *Xcl1*$^{-/-}$ recipients, the pool size of *Xcl1*$^{-/-}$ OT-I T cells, compared to *Xcl1*$^{+/+}$ T cells, was reduced by about 65% already on day 6, and by 60% on day 12 (Figure 6B, bottom row). These experiments demonstrated that secretion of XCL1 has major consequences on the resulting pool size of the CD8+ T cells. At the same time, the reduced

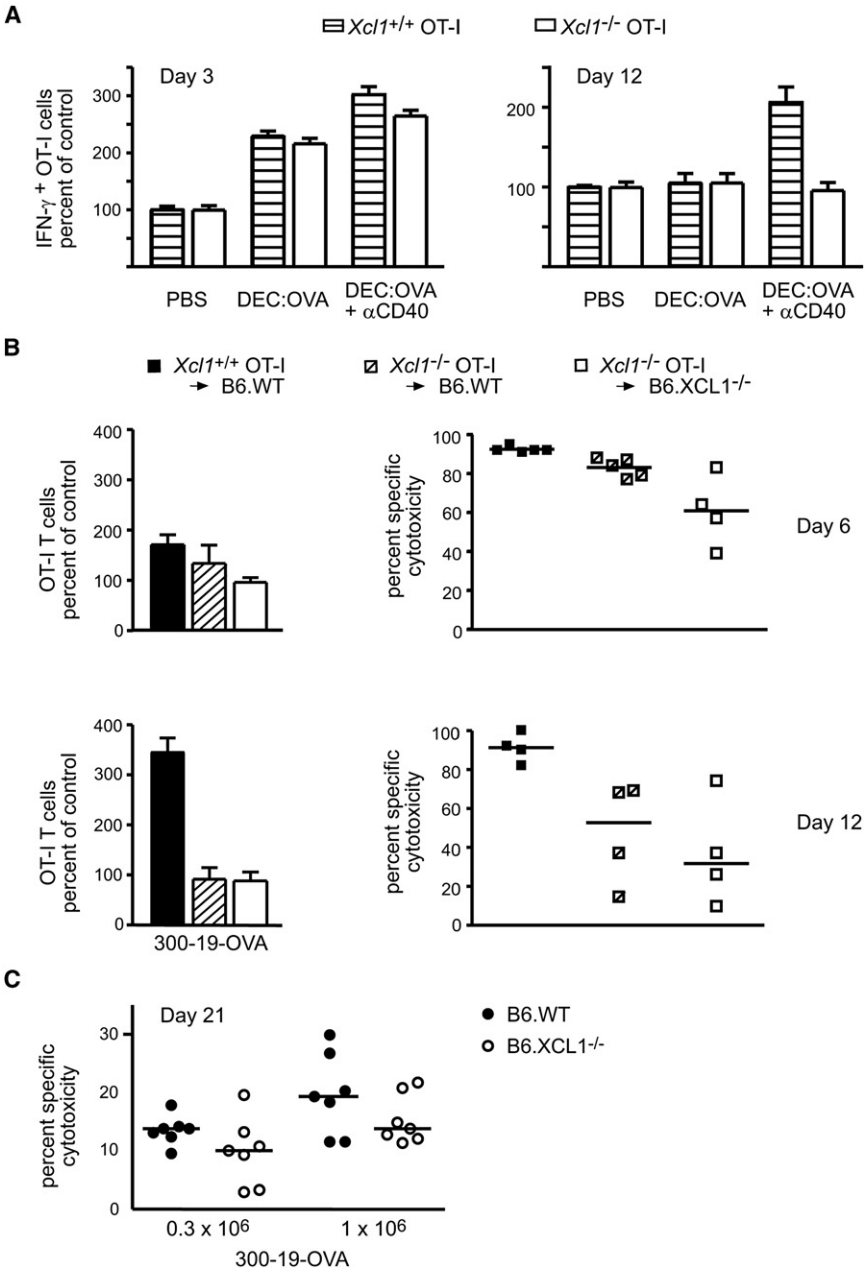

Figure 7. Influence of XCL1 on the Differentiation of CD8+ T Cells to Effector Cells

(A) In the experiment shown in Figure 6A, spleen cells were restimulated in vitro with the SIINFEKL peptide for 5 hr and OT-I T cells were analyzed for intracellular expression of IFN-γ. Shown is the statistical analysis of three experiments (mean ± SEM); the frequencies of $Xcl1^{+/+}$ and $Xcl1^{-/-}$ OT-I T cells capable of secreting IFN-γ after injection with PBS alone were set to 100%.

(B) $Xcl1^{+/+}$ OT-I or $Xcl1^{-/-}$ OT-I T cells were adoptively transferred into wild-type recipients and $Xcl1^{-/-}$ OT-I T cells into $Xcl1^{-/-}$ recipients and the animals were injected 24 hr later with the allogeneic pre B cell line 300-19 transfected with OVA ("300-19-OVA") or with untransfected 300-19 cells (control). The splenic frequencies and the OVA-specific cytotoxic activities of the transferred OT-I T cell populations were determined on days 6 (top row) and 12 (bottom row) after antigen delivery.

(C) The development of endogenous, OVA-specific cytotoxic activity was determined in wild-type and $Xcl1^{-/-}$ animals on day 21 after injection of 300-19-OVA or 300-19 cells on days 1, 3, and 14. Injection of 300-19 cells gave in no instance a cytotoxic activity against OVA-loaded syngeneic target cells. All experiments were performed at least twice. Representative data are shown. Columns are presented as mean ± SEM; bars indicate the median.

expansion of OT-I T cells in *Xcl1*-deficient versus wild-type recipients (around 5-fold versus 15-fold on day 3) indicated a reduced competence of CD8+ DCs for activation of CD8+ T cells in *Xcl1*-deficient mice, at least at the early time points. In these animals, the absence of XCL1 apparently influences the homeostatic activation or differentiation status of CD8+ DCs.

To assess any contribution of XCL1 to the early activation of CD8+ T cells interacting with CD8+ DCs, we transferred $Xcl1^{+/+}$ or $Xcl1^{-/-}$ OT-I T cells into wild-type recipients and compared their activation status at 6, 12, 18, 24, and 48 hr after application of αDEC-205:OVA. Interestingly, we observed that $Xcl1^{-/-}$ OT-I T cells exhibited a differing activation pattern at around 20 hr, with higher expression of CD69, CD25, and 4-1BB (Figure 6C). Although these differences were not dramatic, they were consistently observed in six experiments; at other time points and with other markers (CD27, ICOS, PD-1, OX40, BTLA), no differences were noticed. Similar data were obtained upon additional injection of CD40 mAb (not shown). These experiments suggested that XCL1 modifies the activation status of CD8+ DCs, which in turns changes the activation pattern of the interacting CD8+ T cells.

XCL1 Augments the Capacity of CD8+ T Cells for IFN-γ Secretion and Cytotoxic Activity

To assess the influence of XCL1 on the differentiation of CD8+ T cells to effector cells, we measured the capacity of $Xcl1^{+/+}$ OT-I or $Xcl1^{-/-}$ OT-I T cells to secrete TNF-α, IL-2, and IFN-γ in the system of tolerization and immunization (see Figure 6A). XCL1 did not affect the secretion capacity of either group of OT-I T cells for IFN-γ on day 3 or in tolerized OT-I T cells on day 12 (Figure 7A). However, immunized $Xcl1^{-/-}$ OT-I T cells exhibited a reduced capacity (by an average of 44%) to secrete IFN-γ on day 12 (Figure 7A). No major differences were observed for TNF-α and IL-2 (not shown).

In order to examine the influence of XCL1 on CD8+ T cell differentiation in a system independent of antigen targeting via DEC-205 and costimulation with the CD40 mAb, OVA-transfected allogeneic pre-B cells ("300-19-OVA") were injected i.v. for antigen delivery. In such a system, the antigenic content of the cell line is specifically processed and (cross-) presented by

splenic CD8+ DCs, thus triggering CD8+ T cells to differentiate into cytotoxic cells (Law et al., 1977; den Haan et al., 2000; Iyoda et al. 2002; and our observations). We have examined the influence of XCL1 on the expansion and differentiation of CD8+ T cells under these conditions. *Xcl1*$^{+/+}$ OT-I or *Xcl1*$^{-/-}$ OT-I T cells were adoptively transferred into wild-type recipients and *Xcl1*$^{-/-}$ OT-I T cells into *Xcl1*$^{-/-}$ recipients and the animals were injected 24 hr later with 300-19-OVA cells. No dramatic differences were observed on the frequencies of the OT-I T cells in the spleen on day 6 (Figure 7B, top row). However, 12 days after 300-19-OVA injection, the pool size of *Xcl1*$^{+/+}$ OT-I T cells was several fold higher when compared to *Xcl1*$^{-/-}$ OT-I T cells transferred into wild-type or *Xcl1*$^{-/-}$ recipients (Figure 7B, bottom row). Functionally, a very potent OVA-specific in vivo cytotoxicity could be observed with *Xcl1*$^{+/+}$ OT-I T cells already 6 days after transfer into wild-type recipients, which in tendency was diminished in transferred *Xcl1*$^{-/-}$ T cells (Figure 7B, top row). On day 12, the differences in cytotoxic activity between *Xcl1*$^{+/+}$ and *Xcl1*$^{-/-}$ OT-I T cells became prominent (Figure 7B, bottom row).

The OT-I adoptive transfer system used for the cytotoxicity experiments gives an increased starting frequency of OVA-specific T cells and may for this reason not reflect all aspects of the physiological differentiation of CD8+ T cells into cytotoxic effectors. We have therefore also tested the endogenous cytotoxic response of wild-type and *Xcl1*$^{-/-}$ mice by immunizing them with the 300-19-OVA cell line. When the development of OVA-specific cytotoxicity was tested on day 21 in vivo, *Xcl1*$^{-/-}$ mice again exhibited a reduced response (Figure 7C).

DISCUSSION

In the present work, we provide consistent experimental data for the functional understanding of the chemokine XCL1 and its receptor XCR1. The basis for this advancement is the demonstration of an essentially exclusive expression of XCR1 in murine CD8+ DCs. XCR1-reporter mice revealed an expression of XCR1 in a large majority (70%–85%) of splenic CD8+ DCs, which coexpress CD205 and CD103. We could show that XCL1 induces a calcium flux in CD8+ DCs and acts as a strong and specific chemoattractant for splenic and LN CD8+ DCs; the negative results obtained with *Xcr1*$^{-/-}$ CD8+ DCs in these assays indicated that the chemotactic action of XCL1 is mediated solely through XCR1. Our data show that XCR1+ DCs are located in the red pulp, the marginal zones, and central areas of T cell zones of the spleen and the subcapsular sinus of lymph nodes. In a series of in vivo experiments, we observed that CD8+ T cells secrete XCL1 in a dose-dependent fashion 8–36 hr after encountering antigen on CD8+ DCs. We could demonstrate with two independent systems of antigen targeting into CD8+ DCs that XCL1 secretion substantially increases the survival of CD8+ T cells and their differentiation to IFN-γ-secreting effectors in the first 2 weeks after antigen contact in vivo. Finally and importantly, absence of XCL1 impaired the development of antigen-specific cytotoxicity in vivo.

Both our XCR1 expression data and functional results with XCL1 are at variance with numerous reports in the past. Originally, XCR1 (cloned as orphan receptor GPR5), when transfected into a cell line, has been shown to be the only chemokine receptor capable of mediating a calcium signal and chemotaxis in response to XCL1 (Yoshida et al., 1998, and our unpublished results). The subsequent search for primary cells expressing XCR1 has obviously been hampered by several factors. First, CD8+ DCs represent only a very minor population, approximately 0.2% of splenic cells, which contaminates any isolated cell population unless rigidly removed. Second, all past analyses relied on PCR systems utilizing mRNA and cDNA encoded by exon 2 only. Thus, trace amounts of genomic DNA typically present in total RNA preparations easily resulted in false-positive PCR signals for XCR1 mRNA in many tissues, also in our hands (Dorner et al., 2002). Only the use of polyA-RNA or a qRT-PCR system spanning the intron-exon boundaries of the XCR1 gene eliminated this problem and revealed a selective expression of XCR1 in CD8+ DCs. Finally, immature and LPS-matured bone-marrow-derived DCs, very often used for studies in vitro, do not express XCR1 mRNA (data not shown). The description of XCL1 as a chemokine attracting T cells, B cells, NK cells, and other cell types was already disputed in the past (see Table S1; Dorner et al., 1997; Yoshida et al., 1998; Bleul et al., 1996). The failure to detect XCR1 mRNA in these populations with a highly sensitive assay makes XCL1 an unlikely chemoattractant for these cell populations, unless one would postulate a second receptor for XCL1. There is, however, no evidence for such a second receptor, and the original recognition of XCR1 and XCL1 as a monogamous ligand-receptor system has been confirmed (Yoshida et al., 1998). In fact, we could demonstrate with *Xcr1*$^{-/-}$ cells that XCL1 exerts its chemotaxis on CD8+ DCs exclusively via XCR1. Moreover, in the same assays in which XCL1 exhibited potent chemoattraction on CD8+ DCs, no effect was seen on T cells, B cells, or NK cells.

In the steady state and also after antigen targeting (αDEC-205:OVA ± αCD40) and recognition, XCR1+ DCs, along with other CD11c+ DCs, are located in the same or in neighboring anatomical subregions of spleen and LN as CD8+ T cells, suggesting that XCL1 exerts its function mainly at short distances within immune tissues. It has been proposed that communication between CD8+ T cells and DCs starts with a phase of unstable interactions (around 0–10 hr), and is followed by a phase of prolonged interactions (around 10–20 hr) and another phase of unstable interactions (20–30 hr) (Mempel et al., 2004). The very abundant expression of XCL1 with a peak at 12 hr strongly suggests that the chemokine XCL1 is one of the factors inducing prolonged interactions between CD8+ T cells and CD8+ DCs. A positive correlation between the duration of antigen exposure and the final pool size of antigen-reactive CD8+ T cells (Prlic et al., 2006; Tewari et al., 2006) has recently been demonstrated. XCL1 most likely increases the effective "antigen recognition time" for CD8+ T cells, because absence of XCL1 very substantially reduces the number of surviving antigen-reactive T cells and impairs the development of cytotoxicity. Moreover, XCL1 has the potential to attract neighboring CD8+ DCs to the site of first antigen encounter, because XCR1+ CD8+ DCs are capable of migrating within splenic tissue compartments (our unpublished data); an incoming antigen could thus be taken up and presented by a larger population of CD8+ DCs. XCL1 thus is a candidate factor for the subdomain organization of CD8+ T cell-DC interactions postulated as essential for an efficient immune response (Germain et al., 2008). Moreover, the high

correlation between the strength of the antigenic signal and the amount of secreted XCL1 offers an additional regulatory feedback system. In contrast to the contribution of $CD8^+$ DCs to the regulation of T cell-DC interaction, e.g., induced by Toll-like receptor ligands, such a regulatory loop would be strictly antigen dependent. Together, XCL1 may thus act at multiple points to optimize antigen uptake, processing, and recognition by T cells in cytotoxic Th1 cell immunity.

Independent of its function, the exclusive expression of XCR1 on $CD8^+$ DCs has a number of interesting implications. For first, it allows researchers to develop experimental strategies to delete $CD8^+$ DCs in vivo, either temporally or permanently, and work of this type is under way. Maybe even more intriguing, XCR1 could be used to target antigens to $CD8^+$ DCs. It has been elegantly demonstrated that delivery of antigen to $CD8^+$ DCs via DEC-205 very efficiently induces $CD8^+$ T cell responses (Bonifaz et al., 2002). The loading of $CD8^+$ DCs may be needed to develop potent Th1 cell immunity against certain infections and also tumors, where conventional vaccines (which mainly induce protective antibodies) fail (Figdor et al., 2004). The highly selective expression of XCR1 on $CD8^+$ DCs and the typical internalization of chemokine receptors upon ligand binding make XCR1 a potentially ideal entry port for Th1 cell vaccines.

EXPERIMENTAL PROCEDURES

Cells, Mice, and Adoptive Transfer of T Cells

Cells were isolated, unless indicated otherwise, from C57BL/6 mice. For generation of *Xcl1*-deficient mice, exons 2 and 3 of the *Xcl1* gene were replaced by a neomycin resistance cassette in 129SV embryonic stem cells via the targeting vector pTV-0 (Riethmacher et al., 1995); the remaining intact exon 1 codes only for the signal peptide. *Xcl1*$^{-/-}$ mice were backcrossed to the C57BL/6 background for 10 generations. OT-I TCR-transgenic mice (Hogquist et al., 1994) were crossed onto B6.PL mice to allow identification of adoptively transferred cells with the CD90.1 marker, and further crossed to *Xcl1*-deficient mice. B6.XCR1-lacZ mice were obtained from The Jackson Laboratories. For adoptive transfer experiments, splenocytes from 8- to 10-week-old female donors containing 2.5×10^6 OT-I T cells (unless indicated otherwise) were injected i.v. alone or together with 6 μg of CD40 mAb FGK into female recipients of the same age. All mice were bred under specific-pathogen-free conditions in the animal facility of the Federal Institute for Risk Assessment (Berlin, Germany), and experiments were performed according to state guidelines and approved by the local ethics committee.

Antibodies

Antibodies recognizing CD8 (clone 53-6.72), CD4 (GK1.5), CD19 (1D3), CD11b (5C6), CD11c (N418), and MHC-class II (M5/114.15.2) were from ATCC; CD90.1 (OX-7) from ECACC; F4/80 (BM8), CD69 (H1.2F3), CD3 (145-2C11), Ly-6G/C (RB6-8C5), and CD317 (PDCA-1) from eBioscience; and NK1.1 (PK136) and CD103 (M290) from BD Biosciences. IFN-γ was stained with mAb AN-18 (eBioscience), XCL1 with mAb MTAC-2, generated by immunizing Lewis rats with His-tagged murine XCL1 (Val_{22}-Gly_{114}). αDEC-205 (NLDC-145, CD205) was generously provided by G. Kraal (Amsterdam), αCD40 (FGK) by T. Rolink (Basel), αCD3 (KT3) by H. Savelkoul, αCD25 (2E4) by E. Shevach, and αCD28 (37.51) by J. Allison. Conjugation of LPS-free ovalbumin (Sigma) to αDEC-205 mAb was performed as described (Bonifaz et al., 2004).

Flow Cytometry and Cell Sorting

Adoptively transferred OT-I cells were identified by expression of CD90.1. Staining for surface antigens was performed with directly conjugated antibodies. For intracellular staining of XCL1, spleen cells were incubated in vitro with Brefeldin A (5 μg/ml) for 3 hr, without restimulation; for IFN-γ staining, cells were restimulated in vitro with the peptide SIINFEKL (50 ng/ml) for 5 hr in the presence of Brefeldin A. Cells were then fixed with 2% formaldehyde, washed, incubated in 0.5% saponin, and stained for either cytokine. For LacZ reporter analysis, cells were incubated with fluorescein-di-β-D-galactopyranoside (Invitrogen) according to the manufacturer's instructions. Data were acquired on a LSR II flow cytometer (BD Biosciences) and analyzed with FlowJo (Tree Star Inc.). Flow-sorting of cells was performed on an Aria Cell Sorter (BD Biosciences).

Histological Analysis

Organs from *Xcl1*-deficient mice and B6.XCR1-lacZ$^{+/+}$ mice (LNs, spleen, Peyer's patches, thymus, liver, kidney, intestine, lung, heart, salivary gland, suprarenal gland, brain) were histologically examined and immune cells were extensively analyzed. Organs from both mice showed no obvious developmental defects. For the analysis of β-galactosidase activity, splenic and lymph node tissues from homozygous or heterozygous B6.XCR1-lacZ$^{+/+}$ mice were fixed with 0.1% glutaraldehyde plus 4% paraformaldehyde in PBS for 4 hr at RT, immersed in 10% sucrose overnight, and snap-frozen in 0.9% NaCl. Cryosections were washed 3× with cold PBS (pH 7.4) for 5 min after thawing, incubated with X-Gal staining solution (Sanes et al., 1986) overnight at 37°C, washed 3× with PBS, and counterstained with Neutral Red.

Quantitative PCR

For isolation of total RNA, $CD4^+$ T cells ($CD3^+CD4^+$, 99% pure), $CD8^+$ T cells ($CD3^+CD8^+$, 99%), B cells ($CD19^+$, 95%), and NK cells ($NK1.1^+DX5^+$, 92%) were flow-sorted from spleen cells with a strategy ensuring absence of $CD8^+$ DCs. $CD8^+$ DCs ($CD11c^+$MHC-$II^{hi}CD8^+$, 99%) and $CD8^-$ DCs ($CD11c^+$MHC-$II^{hi}CD8^-$, 99%) were flow-sorted from spleen cells after enrichment on a Nycoprep density gradient (1.077 g/ml, Fresenius Kabi, Norway), pDC ($PDCA\text{-}1^+B220^+CD11^{int}$MHC-$II^{int}$, 99%) after enrichment with PDCA-1 magnetobeads (Miltenyi). $CD4^+$ and $CD8^+$ T cells (10^5 cells in 100 μl complete cell culture medium) were activated for 3 days in 96-well plates (Costar #3366) coated with CD3 mAb (145-2C11) at 0.5 μg/ml and CD28 mAb (37.51) at 4 μg/ml, B cells (8×10^6 in 4 ml) were activated by CD40 mAb (FGK, 10 μg/ml) and LPS (5 μg/ml, Sigma L-6529) at 37°C for 48 hr, NK cells (1.6×10^6 in 5 ml) with recombinant IL-2 (1600 U/ml) at 37°C for 2 days. Immature and LPS-matured bone marrow-derived DCs were generated as described earlier (Lutz et al., 1999). Total RNA was prepared with the High Pure RNA Isolation Kit (Roche Diagnostics), poly(A)RNA with the μMACS mRNA Isolation Kit (Miltenyi). RNA concentration, purity, and integrity were determined on the Agilent 2100 bioanalyzer (Agilent Technologies) and by photometrical reading (NanoDrop 1000). For quantitative determination of XCR1 expression in tissues, 1 μg of total RNA was reverse-transcribed into cDNA with hexamer primers and the AMV Reverse Transcription System (Promega). The cDNA was analyzed by qPCR for its content of XCR1 copies with two different primer probe sets: 5′-CCTACGTGAAACTCTAGCACTGG-3′ (forward, F1), 5′-AAGGCTGTAGAG GACTCCATCTG-3′ (reverse, R1), and 5′-FAM-TACAGACTTGAAACCC-MGB-3′ (probe, P1); this test system allowed detection of ≥200 copies of XCR1 in cDNA reverse-transcribed from 1 μg of total RNA. The second qPCR set was used for analysis of poly(A)RNA: 5′-TGCCTGTGTTGATCTCA GCAC-3′ (forward, F2), 5′-CGGTGGATGGTCATGATGG-3′ (reverse, R2), 5′-FAM-CATCAGCCTCTACAGCAGCATCTTCTTCCT-TAMRA-3′ (probe, P2). Amplification of β2-microglobulin was used as a control: 5′-ATTCACCC CCACTGAGACTGA-3′ (forward), 5′-CTCGATCCCAGTAGACGGTC-3′ (reverse), and 5′-FAM-TGCAGAGTTAAGCATGCCAGTATGGCCG-TAMRA-3′ (probe). To generate a standard for mRNA and cDNA copy quantification, the specific XCR1 gene fragment was amplified and cloned into pJET1.2 with the CloneJET PCR cloning kit (Fermentas). For quantitative PCR, primers were mixed with 10 μl ABsolute QPCR Mix including ROX (ABgene) and 1/10th of the cDNA in a 20 μl PCR-reaction. PCR was performed and quantified on the Mx3000P QPCR System from Stratagene with initial enzyme activation for 15 min at 95°C followed by 40 cycles (95°C, 15 s; 60°C, 1 min). Standard PCR for murine XCR1 was performed with the Phusion Hot Start High-Fidelity DNA Polymerase (Finnzymes) in a 50 μl volume with primers F1 and R1 with initial denaturation for 30 s at 98°C followed by 40 cycles (98°C, 10 s; 60°C, 30 s; 72°C, 30 s) and a 10 min delay at 72°C.

Fluorometric $[Ca^{2+}]_i$ Determination

$CD8^+$ and $CD8^-$ DCs, freshly flow-sorted to a purity >96% with mAb to CD8, CD11b, CD11c, and MHC-class II, were supplemented with 2 μM fura-2/AM

(Molecular Probes) and allowed to settle on poly-L-lysine-coated glass coverslips at 37°C and 5% CO_2 for 30 min in a humidified atmosphere. Adherent cells were superfused with a HEPES-buffered solution containing 128 mM NaCl, 6 mM KCl, 1 mM $MgCl_2$, 1 mM $CaCl_2$, 5.5 mM glucose, 10 mM HEPES, 0.2% BSA, and mounted onto the stage of an inverted microscope (Axiovert 100, Zeiss). During application of 1000 ng/ml XCL1, fura-2 was sequentially excited with monochromatic light of 340 nm, 358 nm, 380 nm, and 480 nm, and fluorescence emission was detected through a 512 nm long pass filter with a cooled CCD-camera (TILL-Photonics), $[Ca^{2+}]_i$ was calculated after spectral unmixing (Lenz et al., 2002).

Chemotaxis Assay

Spleens or popliteal and inguinal LNs of C57/BL6 mice were cut into small pieces and digested with Collagenase D (500 μg/ml) and DNase I (20 μg/ml, both Roche, Mannheim, Germany) for 25 min at 37°C in RPMI 1640 containing 2% FCS (low endotoxin, Biochrom, Berlin, Germany), EDTA (10 mM) was added for additional 5 min and cells were filtered through a 70 μm nylon sieve (BD Falcon). DCs were enriched (purity > 90%) by centrifugation over a Nycoprep density gradient (1.077 g/ml), followed by magnetic cell sorting with αCD11c microbeads (Miltenyi). T cells (>98% $CD3^+$) were magnetically sorted from spleen cells with αCD90 beads, B cells (>97%) with biotinylated CD19 mAb and anti-biotin beads. NK cells (>60% $NK1.1^+$) were obtained by depletion of splenic cells with biotinylated CD3, CD19, and Ly-6G/C mAb, followed by anti-biotin beads (Miltenyi).

For migration assays, cells (0.5–1 × 10^6) suspended in 100 μl chemotaxis medium (RPMI 1640, 1% BSA, 50 μM β-ME, 100 μg/ml penicillin/streptomycin) were placed into the upper chamber of a 24 Transwell system (6.5 mm diameter, 5 μm pore polycarbonate membrane, Corning Costar Co., Acton, MA, USA). The lower chamber was filled with chemotaxis medium containing chemically synthesized murine XCL1 (Dictagene, Lausanne, Switzerland), or any of the control chemokines CCL21, CXCL12, and CXCL9 (all R&D Systems). Cells were incubated for 120–150 min at 37°C in 5% CO_2. The cells in the lower chamber were analyzed by flow cytometry for the expression of CD8, CD11b, and CD11c (DCs), CD3 (T cells), CD19 (B cells), and NK1.1 (NK cells). The absolute number of input or migrated cells was determined by counting cells in a defined volume via a flow cytometer. The percentage of migrated cells was calculated by dividing the number of cells in the lower chamber by the number of input cells (number migrated cells/number input cells × 100). All experiments were performed with duplicate wells.

Ovalbumin-Expressing Cell Line

The cDNA encoding amino acids 138–386 of OVA ("ΔOVA") was cloned in-frame with the Yellow Fluorescent Protein into the pcDNA3 vector (Invitrogen) and verified by sequencing. A stable line expressing the truncated, nonsecreted form of OVA ("300-19-OVA") was obtained with the ΔOVA-YFP-pcDNA3 vector by electroporation of the pre-B cell line 300-19 (Alt et al., 1981), followed by subcloning of YFP-expressing cells under limiting dilution conditions.

In Vivo Cytotoxicity Assay

For cytotoxicity assays in the adoptive transfer system, *Xcl1*$^{+/+}$ or *Xcl1*$^{-/-}$ OT-I T cells (1 × 10^6) from female mice were transferred into female recipients, which were injected 24 hr later with 300-19 or 300-19-OVA cells (3 × 10^6) i.v. For induction of endogenous cytotoxicity, animals were repeatedly injected with 300-19 or 300-19-OVA cells (0.3 or 1 × 10^6) i.v. After the indicated immunization periods, the in vivo cytotoxicity assay was performed. To this end, splenocytes from female wild-type C57BL/6 mice were incubated at 30 × 10^6 cells/ml in complete RPMI medium alone or with SIINFEKL peptide (10 μg/ml) for 2 hr. The cells were washed and incubated at 50 × 10^6 cells/ml in the dark with CFSE (Molecular Probes Europe, Breda), either at 1.5 μM (unpulsed cells; $CFSE^{lo}$) or 15 μM (peptide-pulsed cells; $CFSE^{hi}$) for 15 min at 37°C, washed, and resuspended in PBS at 100 × 10^6 cells/ml. Twenty million cells of a 1:1 mixture of $CFSE^{lo}$:$CFSE^{hi}$ were adoptively transferred into test mice, and 18 hr later the splenocytes of test mice were analyzed by flow cytometry. The percentage of target cell killing was calculated with the formula: 100 − (((% relevant peptide-pulsed in immunized/% irrelevant peptide-pulsed in immunized)/(% relevant peptide-peptide pulsed in control/% irrelevant peptide-pulsed in control)) × 100). The injection of untransfected 300-19 cells gave in no instance a signal in the OVA-specific cytotoxicity assay.

SUPPLEMENTAL DATA

Supplemental Data include four tables and can be found with this article online at http://www.cell.com/immunity/supplemental/S1074-7613(09)00455-5.

ACKNOWLEDGMENTS

The expert technical assistance of E. Kowalczyk and M. Jaensch is gratefully acknowledged, and we thank J. Löhler for histological analysis of *Xcl1*-deficient mice. We are grateful to M. Lutz for generation of bone marrow-derived DCs. This work was supported by grants from the Deutsche Forschungsgemeinschaft to R.A.K. (SFB421) and in part by the Wilhelm Sander-Stiftung.

Received: July 24, 2008
Revised: June 18, 2009
Accepted: August 21, 2009
Published online: November 12, 2009

REFERENCES

Alt, F., Rosenberg, N., Lewis, S., Thomas, E., and Baltimore, D. (1981). Organization and reorganization of immunoglobulin genes in A-MULV-transformed cells: rearrangement of heavy but not light chain genes. Cell *27*, 381–390.

Bleul, C.C., Fuhlbrigge, R.C., Casasnovas, J.M., Aiuti, A., and Springer, T.A. (1996). A highly efficacious lymphocyte chemoattractant, stromal cell-derived factor 1 (SDF-1). J. Exp. Med. *184*, 1101–1109.

Bonifaz, L., Bonnyay, D., Mahnke, K., Rivera, M., Nussenzweig, M.C., and Steinman, R.M. (2002). Efficient targeting of protein antigen to the dendritic cell receptor DEC-205 in the steady state leads to antigen presentation on major histocompatibility complex class I products and peripheral $CD8^+$ T cell tolerance. J. Exp. Med. *196*, 1627–1638.

Bonifaz, L.C., Bonnyay, D.P., Charalambous, A., Darguste, D.I., Fujii, S., Soares, H., Brimnes, M.K., Moltedo, B., Moran, T.M., and Steinman, R.M. (2004). In vivo targeting of antigens to maturing dendritic cells via the DEC-205 receptor improves T cell vaccination. J. Exp. Med. *199*, 815–824.

den Haan, J.M., Lehar, S.M., and Bevan, M.J. (2000). $CD8^+$ but not $CD8^-$ dendritic cells cross-prime cytotoxic T cells in vivo. J. Exp. Med. *192*, 1685–1696.

Dorner, B., Müller, S., Entschladen, F., Schröder, J.M., Franke, P., Kraft, R., Friedl, P., Clark-Lewis, I., and Kroczek, R.A. (1997). Purification, structural analysis, and function of natural ATAC, a cytokine secreted by $CD8^+$ T cells. J. Biol. Chem. *272*, 8817–8823.

Dorner, B.G., Scheffold, A., Rolph, M.S., Hüser, M.B., Kaufmann, S.H., Radbruch, A., Flesch, I.E., and Kroczek, R.A. (2002). MIP-1α, MIP-1β, RANTES, and ATAC/lymphotactin function together with IFN–γ as type 1 cytokines. Proc. Natl. Acad. Sci. USA *99*, 6181–6186.

Dorner, B.G., Smith, H.R., French, A.R., Kim, S., Poursine-Laurent, J., Beckman, D.L., Pingel, J.T., Kroczek, R.A., and Yokoyama, W.M. (2004). Coordinate expression of cytokines and chemokines by NK cells during murine cytomegalovirus infection. J. Immunol. *172*, 3119–3131.

Figdor, C.G., de Vries, I., Lesterhuis, W.J., and Melief, C.J. (2004). Dendritic cell immunotherapy: Mapping the way. Nat. Med. *10*, 475–480.

Germain, R.N., Bajenoff, M., Castellino, F., Chieppa, M., Egen, J.G., Huang, A.Y., Ishii, M., Koo, L.Y., and Qi, H. (2008). Making friends in out-of-the-way places: how cells of the immune system get together and how they conduct their business as revealed by intravital imaging. Immunol. Rev. *221*, 163–181.

Heath, W.R., Belz, G.T., Behrens, G.M., Smith, C.M., Forehan, S.P., Parish, I.A., Davey, G.M., Wilson, N.S., Carbone, F.R., and Villadangos, J.A. (2004). Cross-presentation, dendritic cell subsets, and the generation of immunity to cellular antigens. Immunol. Rev. *199*, 9–26.

Hogquist, K.A., Jameson, S.C., Heath, W.R., Howard, J.L., Bevan, M.J., and Carbone, F.R. (1994). T cell receptor antagonist peptides induce positive selection. Cell *76*, 17–27.

Huang, A.Y., Golumbek, P., Ahmadzadeh, M., Jaffee, E., Pardoll, D., and Levitsky, H. (1994). Role of bone marrow-derived cells in presenting MHC class I-restricted tumor antigens. Science *264*, 961–965.

Idoyaga, J., Suda, N., Suda, K., Park, C.G., and Steinman, R.M. (2009). Antibody to Langerin/CD207 localizes large numbers of CD8α^+ dendritic cells to the marginal zone of mouse spleen. Proc. Natl. Acad. Sci. USA *106*, 1524–1529.

Iyoda, T., Shimoyama, S., Liu, K., Omatsu, Y., Akiyama, Y., Maeda, Y., Takahara, K., Steinman, R.M., and Inaba, K. (2002). The CD8$^+$ dendritic cell subset selectively endocytoses dying cells in culture and in vivo. J. Exp. Med. *195*, 1289–1302.

Kelner, G.S., Kennedy, J., Bacon, K.B., Kleyensteuber, S., Largaespada, D.A., Jenkins, N.A., Copeland, N.G., Bazan, J.F., Moore, K.W., Schall, T.J., and Zlotnik, A. (1994). Lymphotactin: A cytokine that represents a new class of chemokine. Science *266*, 1395–1399.

Kennedy, J., Kelner, G.S., Kleyensteuber, S., Schall, T.J., Weiss, M.C., Yssel, H., Schneider, P.V., Cocks, B.G., Bacon, K.B., and Zlotnik, A. (1995). Molecular cloning and functional characterization of human lymphotactin. J. Immunol. *155*, 203–209.

Law, L.W., Takemoto, K.K., Rogers, M.J., and Ting, R.C. (1977). Induction of Simian virus 40 (SV40) transplantation immunity in mice by SV40-transformed cells of various species. J. Natl. Cancer Inst. *59*, 1523–1526.

Lenz, J.C., Reusch, H.P., Albrecht, N., Schultz, G., and Schaefer, M. (2002). Ca^{2+}-controlled competitive diacylglycerol binding of protein kinase C isoenzymes in living cells. J. Cell Biol. *159*, 291–302.

Lutz, M.B., Kukutsch, N., Ogilvie, A.L.J., Rößner, S., Koch, F., Romani, N., and Schuler, G. (1999). An advanced culture method for generating large quantities of highly pure dendritic cells from bone marrow. J. Immunol. Methods *223*, 77–92.

McLellan, A.D., Kapp, M., Eggert, A., Linden, C., Bommhardt, U., Bröcker, E.B., Kämmerer, U., and Kämpgen, E. (2002). Anatomic location and T-cell stimulatory functions of mouse dendritic cell subsets defined by CD4 and CD8 expression. Blood *99*, 2084–2093.

Mempel, T.R., Henrickson, S.E., and von Andrian, U.H. (2004). T-cell priming by dendritic cells in lymph nodes occurs in three distinct phases. Nature *427*, 154–159.

Müller, S., Dorner, B., Korthäuer, U., Mages, H.W., D'Apuzzo, M., Senger, G., and Kroczek, R.A. (1995). Cloning of ATAC, an activation-induced, chemokine-related molecule exclusively expressed in CD8$^+$ T lymphocytes. Eur. J. Immunol. *25*, 1744–1748.

Prlic, M., Hernandez-Hoyos, G., and Bevan, M.J. (2006). Duration of the initial TCR stimulus controls the magnitude but not functionality of the CD8$^+$ T cell response. J. Exp. Med. *203*, 2135–2143.

Riethmacher, D., Brinkmann, V., and Birchmeier, C. (1995). A targeted mutation in the mouse E-cadherin gene results in defective preimplantation development. Proc. Natl. Acad. Sci. USA *92*, 855–859.

Sanes, J.R., Rubenstein, J.L., and Nicolas, J.F. (1986). Use of a recombinant retrovirus to study post-implantation cell lineage in mouse embryos. EMBO J. *5*, 3133–3142.

Tewari, K., Walent, J., Svaren, J., Zamoyska, R., and Suresh, M. (2006). Differential requirement for Lck during primary and memory CD8$^+$ T cell responses. Proc. Natl. Acad. Sci. USA *103*, 16388–16393.

Vremec, D., Pooley, J., Hochrein, H., Wu, L., and Shortman, K. (2000). CD4 and CD8 expression by dendritic cell subtypes in mouse thymus and spleen. J. Immunol. *164*, 2978–2986.

Yoshida, T., Imai, T., Kakizaki, M., Nishimura, M., Takagi, S., and Yoshie, O. (1998). Identification of single C motif-1/lymphotactin receptor XCR1. J. Biol. Chem. *273*, 16551–16554.

Yoshida, T., Imai, T., Kakizaki, M., Nishimura, M., and Yoshie, O. (1995). Molecular cloning of a novel C or gamma type chemokine, SCM-1. FEBS Lett. *360*, 155–159.

Zlotnik, A., and Yoshie, O. (2000). Chemokines: A new classification system and their role in immunity. Immunity *12*, 121–127.